

Zero-temperature series expansions for the Kondo lattice model at half filling

Weihong Zheng* and J. Oitmaa†

School of Physics, The University of New South Wales, Sydney NSW 2052, Australia

(Received 11 September 2002; published 6 June 2003)

We present results for the Kondo lattice model of strongly correlated electrons, in one, two, and three dimensions, obtained from high-order linked-cluster series expansions. Results are given for various ground-state properties at half filling, and for spin and charge excitations. Estimates for the location of the quantum critical point in the square and simple cubic lattices are made.

DOI: 10.1103/PhysRevB.67.214406

PACS number(s): 71.10.Fd, 71.27.+a

I. INTRODUCTION

The Kondo lattice model (KLM), described by the usual Hamiltonian

$$H = -t \sum_{\langle ij \rangle \sigma} (c_{i\sigma}^\dagger c_{j\sigma} + \text{H.c.}) + J \sum_i \mathbf{S}_i \cdot \mathbf{s}_i, \quad (1)$$

represents a band of conduction electrons, interacting via a spin-exchange term with a set of immobile $s = \frac{1}{2}$ spins \mathbf{S}_i (f electrons).

The model has been extensively studied in connection with a class of materials known as “Kondo insulators” ($J > 0$),^{1,2} and in connection with the manganites ($J < 0$).³ Despite the apparent simplicity of the model, in which neither the conduction electrons nor the localized spins interact directly among themselves, the spin exchange leads to a strongly correlated many-body system. No exact results are known for either ground-state or thermodynamic properties for general J/t , in any dimension.

The model incorporates two competing physical processes. In the strong-coupling (large $|J|$) limit, the conduction electrons are “frozen out” via the formation of local singlets ($J > 0$) or triplets ($J < 0$). In either case there will be a gap to spin excitations and spin correlations will be short ranged. On the other hand, at weak coupling, the conduction electrons can induce the usual RKKY interaction between localized spins, giving rise to possible magnetically ordered phases with no spin gap and long-range correlations. In one dimension there will be a smooth crossover from large $|J|$ to small $|J|$ behavior, but in higher dimension a quantum phase transition is expected.

There is a considerable interest in the model in connection with experiments on heavy fermion materials, where anomalous behavior is seen in the vicinity of the antiferromagnetic quantum critical point.⁴ A popular scenario,⁵ within the context of the Kondo lattice model, invokes the role of antiferromagnetic spin fluctuations coupling to the Fermi liquid properties. While we do not address this connection here, we hope our results may be of some relevance in this area.

A great deal of work has been carried out on the one-dimensional model, using a variety of analytic and numerical methods, and we refer the reader to a recent review.⁶ In higher dimension there have been mean-field approaches,⁷⁻⁹ quantum Monte Carlo calculations,¹⁰ and a series expansion study.¹¹ These studies, which are all for the half filled case,

conclude that a quantum phase transition, at which the spin gap vanishes continuously, occurs at $(J/t)_c \approx 1.45 \pm 0.05$ in the 2D $J > 0$ case, while Refs. 9 and 11 give $(J/t)_c \approx 1.833$ and 2.0, respectively, for the 3D $J > 0$ case. There have not been, to the best of our knowledge, any similar studies for the case of ferromagnetic coupling.

Our aim in this paper is to study the Kondo lattice model in one, two, and three dimensions via series expansion methods. We have considerably extended the calculations of Ref. 11, by obtaining longer series, by using also expansions about the Ising limit, and by studying also the energies of elementary excitations.

Linked-cluster series expansions have been used successfully for many years to study strongly interacting lattice models. A recent review¹² describes the basic approach and some of the results which have been obtained. The method is applicable in any dimension, is particularly suited to locating critical points, and is free from finite-size corrections or minus sign problems which hamper other numerical approaches. On the other hand, a good convergence may be limited to particular regions of the phase diagram.

The Hamiltonian is written in the generic form $H = H_0 + \lambda V$, where H_0 has a simple known ground state. The remaining term(s) in H are treated perturbatively, to high order. In this way the ground-state energy, correlations, susceptibilities, etc., are expressed as power series in λ . These are then analyzed by standard methods.¹³ An extension of the basic linked-cluster method^{12,14} allows the computation of the full dispersion relation for elementary excitations, which can yield energy gaps.

For the present model, the simplest choice is to take $H_0 = J \sum_i \mathbf{S}_i \cdot \mathbf{s}_i$, a sum of single-site exchange terms. The unperturbed ground state is then a simple product state of dimer states. This is the approach used in Ref. 11, and also our first method here. We refer to these as “dimer expansions.” An alternative is to write the exchange term as

$$J \sum_i \left[S_i^z s_i^z + \frac{1}{2} (S_i^+ s_i^- + S_i^- s_i^+) \right] \quad (2)$$

and to take only the first term as H_0 . In such an “Ising expansion” both the spin-fluctuation and hopping terms are treated perturbatively. To remove the degeneracy in H_0 , we add following two terms for conduction spins into H_0 :

$$J' \sum_{\langle ij \rangle} (s_i^z s_j^z + 1/4) + h \sum_i [(-1)^i s_i^z + 1/2] \quad (3)$$

and subtract them from the perturbation term, so the overall Hamiltonian is

$$H = H_0 + \lambda V \quad (4)$$

$$H_0 = J \sum_i (S_i^x S_i^x + S_i^y S_i^y) + J' \sum_{\langle ij \rangle} (s_i^z s_j^z + 1/4) + h \sum_i [(-1)^i s_i^z + 1/2] \quad (5)$$

$$V = J \sum_i (S_i^x s_i^x + S_i^y s_i^y) - J' \sum_{\langle ij \rangle} (s_i^z s_j^z + 1/4) - h/2 \sum_i [(-1)^i s_i^z + 1/2] - t \sum_{\langle ij \rangle \sigma} (c_{i\sigma}^+ c_{j\sigma} + \text{H.c.}). \quad (6)$$

Series in power of λ are computed for given values of J, t, J' , and h , and extrapolated to $\lambda = 1$ where the original Hamiltonian is recovered. Such expansions are appropriate for magnetically ordered phases, although they can also yield accurate results in other cases. It must be stressed that, in both forms of expansion, the unperturbed ground state has a conduction electron at each site, and the perturbation conserves electron number. Thus, the system is at half filling. There is no simple way to include the doped case within this formalism.

In the remainder of this paper, we will present and discuss our results for the one-dimensional (1D) case (Sec. II), for the 2D square lattice, and for the 3D simple cubic lattice (Sec. III). An overall summary is given at the end.

II. THE 1D KONDO LATTICE MODEL

Using the dimer expansion approach, we have computed series for the ground-state energy in the form

$$E_0/NJ = \sum_{s=0}^{\infty} e_s (t/J)^s \quad (7)$$

and the coefficients, to order 20, are given in the Appendix. Our coefficients agree exactly with Ref. 11, and add three new terms (odd coefficients vanish for this series). Integrated differential approximants¹³ are used to evaluate the series for particular t/J , and the resulting energy is shown in Fig. 1. The different approximants agree well up to $t/J \approx 1.2$, but then splay outwards. We also show, for a comparison, the energy obtained from an early DMRG calculation.¹⁵

Next we turn to the spin excitations. In the strong-coupling limit, a spin excitation corresponds to a spin triplet at one site, which is able to propagate coherently via the conduction electron hopping term. The dispersion relation can be expressed in the form

$$\Delta_s(k) = \sum_n t_n(\lambda) \cos nk, \quad (8)$$

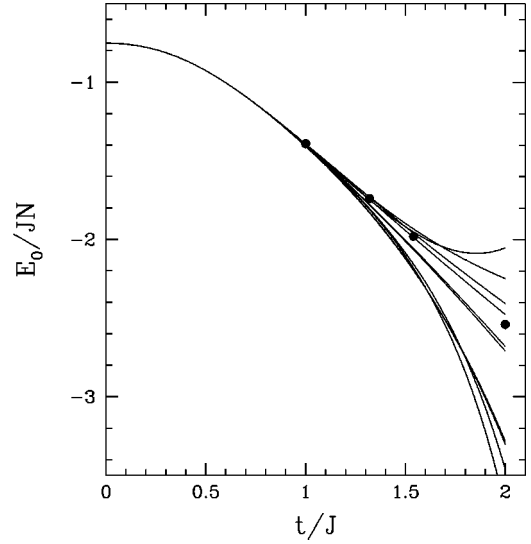


FIG. 1. The ground-state energy for the one-dimensional (1D) Kondo lattice model. The lines represent different approximants to the series. The solid points are the DMRG results (Ref. 15).

where the quantities $t_n(\lambda)$ are expressed as power series in $\lambda = t/J$. For the 1D case we have computed these up to $n = 9$ (order 18 in λ), and for the interested reader we provide this data in the Appendix. Figure 2(a) shows the triplet spin-excitation energy versus k , for value of $t/J = 0.25, 0.4, 0.5$. For $t/J = 0$ the excitation will, of course, have energy J and will be dispersionless. Increasing the hopping amplitude gives increasing bandwidth, with the energy at $k = 0$ raised slightly and a minimum at $k = \pi$. We are unaware of any previous reported calculations of this dispersion relation, apart from the second-order result given in Ref. 6.

It is worth noting that the error bars shown in Fig. 2, and in subsequent figures, represent “confidence limits” only, based on the degree of convergence among different approximants. The large error bars near $k = 0$ for the largest t/J in Fig. 2(a) reflect the irregularity of the corresponding series.

From Eq. (8) at $k = \pi$, we obtain a series in λ for the spin gap, which is again evaluated using integrated differential approximants. Results are shown in Fig. 3. The series is well converged up to $t/J \approx 1.1$. For a comparison, we show spin gaps calculated by DMRG calculation (Ref. 16) and a mean-field approach.¹⁷ Agreement with DMRG is excellent over the range shown, while the mean-field method appear to seriously underestimate the size of the gap. All of the results, including ours, are consistent with a spin gap that decreases rapidly, but does not vanish until $J = 0$.

Next, we consider the so-called “quasiparticle” excitation, which we prefer to call a one-hole excitation. This corresponds to the removal of an electron from the half-filled band and thus, in the strong-coupling limit, to a single localized spin on one site with singlets on the others. For $t = 0$, the energy gap is thus $3J/4$. For the 1D case, we have computed this series up to order 12 in λ . Figure 2(b) shows the one-hole excitation spectrum for values $t/J = 0.25, 0.4$, and 0.5 . The minimum occurs at $k = 0$ and the bandwidth seems roughly proportional to t/J . We are, again, not aware of any previous calculations of this dispersion curve. The series at

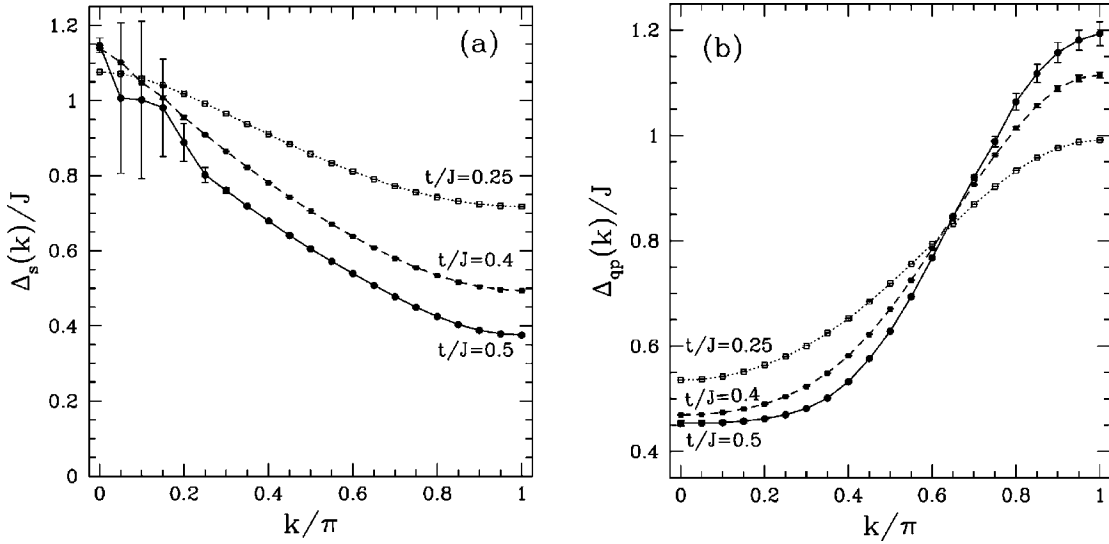


FIG. 2. The triplet spin excitation spectrum (a) and one-hole (quasiparticle) excitation spectrum (b) for 1D case.

$k=0$ allow us to compute the one-hole gap, and our results are plotted in Fig. 3. A notable feature is that Δ_{qp} becomes approximately constant for $t/J > 0.5$. We know of no previous calculations for the one-hole gap apart, again, from the second-order strong-coupling result in Ref. 6. There is yet another gap, the “charge gap,” which corresponds to an excitation in which the system remains half filled, but with a doubly occupied site and an empty site. We are not able to compute this via series, at this stage. However, in the strong-coupling limit $\Delta_c = 2\Delta_{qp}$ (this is valid⁶ to at least second order in t/J). The charge gap has been computed by DMRG calculation,¹⁶ and we show in Fig. 3, the result for $\Delta_c/2$. Evidently, for larger hopping parameter $\Delta_c/\Delta_{qp} < 2$.

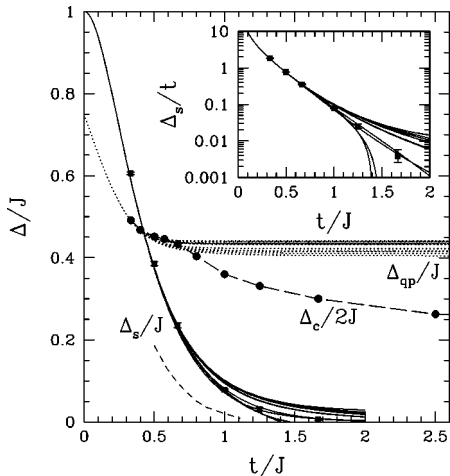


FIG. 3. The triplet spin gap Δ_s/J and quasiparticle gap Δ_{qp}/J vs t/J obtained from different integrated differential approximants. The points are the results of density matrix renormalization group (DMRG) calculation (Ref. 16) for Δ_s/J (points with errorbars) and $\Delta_c/2J$ (solid circles). The short dashed line is the result of a mean-field approach (Ref. 17). The inset gives a logarithmic plot for Δ_s/t .

III. THE SQUARE AND SIMPLE CUBIC LATTICES

In two or more spatial dimensions, it is believed that the Kondo lattice model has a true quantum phase transition at some $(J/t)_c$, between a gapped spin-liquid phase and a small J magnetically ordered gapless phase. For the square lattice, quantum Monte Carlo simulations¹⁰ provide strong indications of a transition at $(t/J)_c \approx 0.69$, while a bond-operator mean-field theory⁹ gives $(t/J)_c = 0.664$ and 0.546 for the square and simple cubic lattices, respectively. A previous series study¹¹ has given $(t/J)_c \approx 0.7$ and 0.5 , respectively. These latter estimates are relatively imprecise, and it seemed worthwhile to investigate this using longer series.

We have derived dimer series for the square lattice for the following quantities: ground-state energy E_0 , antiferromagnetic spin susceptibilities for both local and conduction spins (χ_l and χ_c), and the triplet spin excitation spectrum (all to order 12), and the one-hole (“quasiparticle”) excitation spectrum (to order 11). This adds two nonzero terms to the results of Ref. 11. The excitation series are new. In addition, we have computed Ising expansions for the ground-state energy and for the staggered magnetizations (for both local and itinerant spins) to order 13. Series, to the same order, have been derived for the simple cubic lattice for all of the same quantities, except for the excitations, where we have only computed the minimum gap rather than the full spectrum. The dimer series for ground-state energy E_0 , antiferromagnetic spin susceptibilities for both local and conduction spins (χ_l and χ_c), and the minimum triplet spin gap are given in Table I. Our results agree completely with those of Ref. 11 for the square lattice but disagree for the simple cubic lattice susceptibilities beyond the fourth term. We have been unable to resolve this with the authors of Ref. 11, but we are confident that our results are correct.

We first show, in Fig. 4, our estimate of the ground-state energy, as a function of t , obtained from both dimer and Ising expansions. Both series converge well for small t , but the Ising expansion has better convergence for larger t . There are

TABLE I. Series coefficients for dimer expansions for the ground energy per site E_0/JN , the minimum triplet spin gap Δ_s/J , and the antiferromagnetic spin susceptibilities for both local and conduction spins (χ_l and χ_c). Nonzero coefficients $(t/J)^n$ up to order $n=12$ for square lattice and simple cubic lattice are listed.

n	E_0/JN	Δ_s/J	χ_c	χ_l
square lattice				
0	$-7.500000000 \times 10^{-1}$	1.000000000	$5.000000000 \times 10^{-1}$	$5.000000000 \times 10^{-1}$
2	-1.333333333	-1.333333333×10^1	1.777777778	6.518518519
4	$-8.888888889 \times 10^{-2}$	1.611851852×10^2	4.632888889	3.850916872×10^1
6	4.231487360	-2.640795767×10^2	6.236968731	4.067531551×10^1
8	-1.519899530×10^1	-1.072124632×10^5	4.340134129×10^1	6.687413797×10^1
10	$8.900723089 \times 10^{-1}$	5.495699137×10^6	1.004232541×10^2	1.823289007×10^3
12	3.109971534×10^2	-1.561259011×10^8	-6.384897515×10^2	-4.654864554×10^3
simple cubic lattice				
0	$-7.500000000 \times 10^{-1}$	1.000000000	$5.000000000 \times 10^{-1}$	$5.000000000 \times 10^{-1}$
2	-2.000000000	-2.000000000×10^1	2.666666667	9.777777778
4	$6.666666667 \times 10^{-1}$	3.063111111×10^2	1.291555556×10^1	8.443753086×10^1
6	7.834807760	1.060237771×10^3	5.132587514×10^1	2.399390035×10^2
8	-7.114791245×10^1	-2.760658123×10^5	3.510946982×10^2	1.684588635×10^3
10	3.498368486×10^2	3.860398011×10^6	1.354232378×10^3	1.217247537×10^4
12	-1.603723348×10^2	5.557190900×10^8	2.797156237×10^3	-2.514875289×10^4

no previously reported data for E_0 . There is no evidence of any anomaly in E_0 at the supposed phase transition point, nor would we expect this.

The most direct way of identifying any critical point $(t/J)_c$ is from poles of Dlog Padé approximants.¹³ However the series are irregular (Table I) and, perhaps not surprisingly, this yields no consistent results. However if we know, or assume, the value of the critical exponent γ then biased estimates of the critical point can be obtained from direct Padé approximants to the series for $\chi^{1/\gamma}$, which should have a simple pole. Here, we expect the transition for the square lattice to be of the same universality class as the $d=3$ classical Heisenberg model with $\gamma \approx 1.4$, and for the simple cu-

bic lattice to be of the $d=4$ universality class with $\gamma=1.0$. In Table II we show estimates of x_c^2 ($x=t/J$) obtained in this way. As can be seen, a number of consistent estimates of the pole are obtained, particularly for the series for the conduction electron susceptibility. We might reasonably estimate for the square lattice $(t/J)_c=0.68 \pm 0.02$, and for the simple cubic lattice $(t/J)_c=0.46 \pm 0.01$, where the error are subjective confidence limits. These correspond to $(J/t)_c=1.48$, and 2.15 for the 2D and 3D cases, values which are consistent with previous estimates.

An alternative approach is to evaluate the staggered magnetization and susceptibility directly via integrated differential approximants and to look at the behavior as a function of

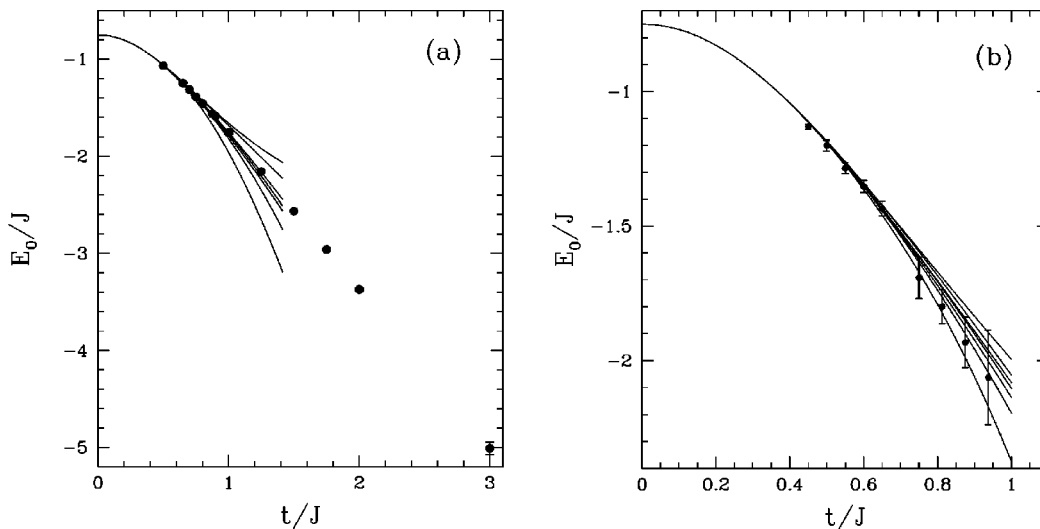


FIG. 4. The ground-state energy for the square lattice (a) and for simple cubic lattice (b). The solid lines are different orders of integrated differential approximants to the dimer expansion series, while the points with errorbars are the results from Ising expansions.

TABLE II. Estimates of $x_c^2 = (t/J)_c^2$ from poles of $[N,D]$ Padé approximants to the series for $\chi_{c,l}^{1/\gamma}$. The index c,l denote the series for conduction electron, localized spin, respectively.

Square Lattice	Approximant	x_c^2	Approximant	x_c^2
$\gamma=1.4$	$[2,3]_c$	0.45378	$[3,3]_c$	0.46298
	$[3,3]_l$	0.46990	$[2,4]_c$	0.46350
	Estimate $x_c^2 = 0.46 \pm 0.02$, $(t/J)_c = 0.68 \pm 0.02$			
Simple Cubic Lattice	Approximant	x_c^2	Approximant	x_c^2
$\gamma=1.0$	$[1,1]_c$	0.20647	$[0,2]_c$	0.20888
	$[2,2]_c$	0.21660	$[2,2]_l$	0.21637
	$[1,3]_c$	0.22094	$[3,2]_c$	0.19300
	$[2,3]_c$	0.20601	$[4,2]_c$	0.19480
	$[3,3]_c$	0.20798	$[3,3]_l$	0.20078
	$[2,4]_c$	0.20809		
	Estimate $x_c^2 = 0.21 \pm 0.01$, $(t/J)_c = 0.46 \pm 0.01$			

t/J . The staggered magnetizations shown in Fig. 5 are obtained from an Ising expansions, starting from an antiferromagnetically ordered state. These are relatively constant for $t/J > 1$, but drop sharply to zero around $t/J \sim 0.6-0.7$ in 2D case and $t/J \sim 0.5$ in 3D case, confirming the existence of a transition to a magnetically disordered phase. The error limits are rather large, and it is not possible to determine the transition point with high precision in this way. Our magnetization curves in 2D are very similar to the Quantum Monte Carlo (QMC) results,¹⁰ although our conduction electron magnetization is much smaller. We show the QMC results for a comparison. In Fig. 6 we show curves of the inverse susceptibilities, in the Kondo phase, obtained from dimer expansions. Again, there is a clear evidence for the transition, but it is difficult to locate precisely. Our best estimates from these figures would be $t/J \approx 0.75 \pm 0.10$ in 2D case and $t/J \approx 0.50 \pm 0.05$ in 3D case, less precise but quite consistent

with the direct Padé approximant estimates.

Next, we consider the spin triplet and one-hole (quasiparticle) excitations. Figure 7(a) shows the full spin triplet dispersion curve for $t/J = 0.25, 0.4$, both in the Kondo phase, for 2D case. For comparison we also show variational Monte Carlo results of Wang *et al.*¹⁸ The lowest spin excitation is at (π, π) , and the spin gap clearly decreases as t increases.

In Fig. 7(b) we show the dispersion relation for the one-hole excitation, again for $t/J = 0.25, 0.4$, for the 2D case. The minimum occurs at $\mathbf{k} = (0,0)$, with a maximum at (π, π) . The overall shape is qualitatively similar to the mean-field results of Ref. 9. We note the large error bars near (π, π) for $t/J = 0.4$.

Series have also been computed directly for the spin gap and quasiparticle gap, for both 2D and 3D cases. Analysis is shown in Fig. 8. The data clearly show the spin gap decreasing to zero at a critical point $(t/J)_c$, the position being con-

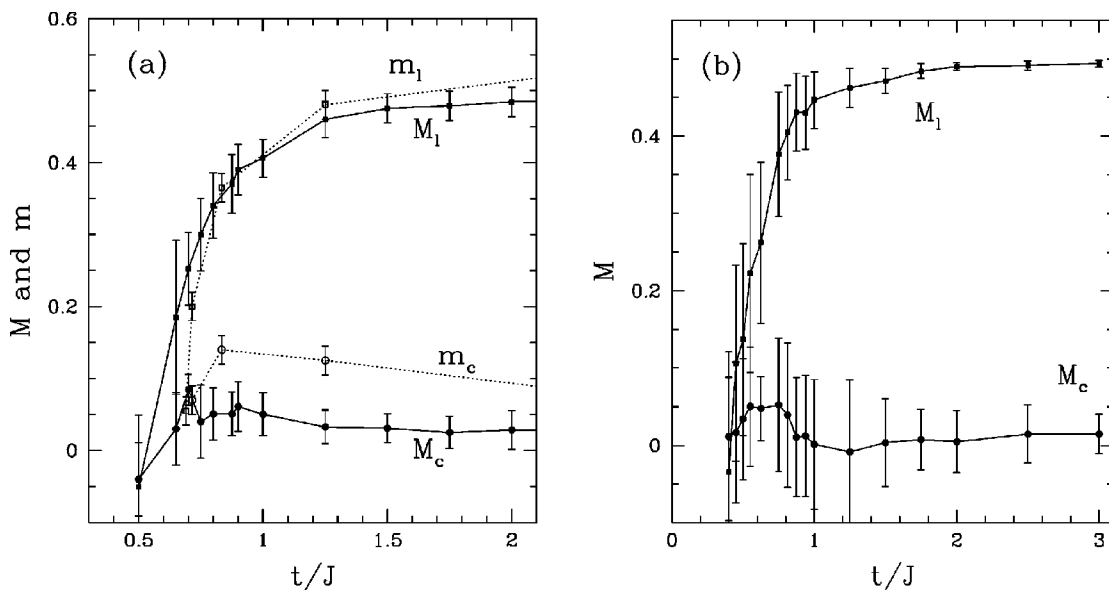


FIG. 5. The staggered magnetizations for both localized spins (M_l) and conduction electrons (M_c) for the square lattice (a) and for simple cubic lattice (b). Also shown for square lattice are the staggered moments m obtained from Monte Carlo calculations (Ref.10).

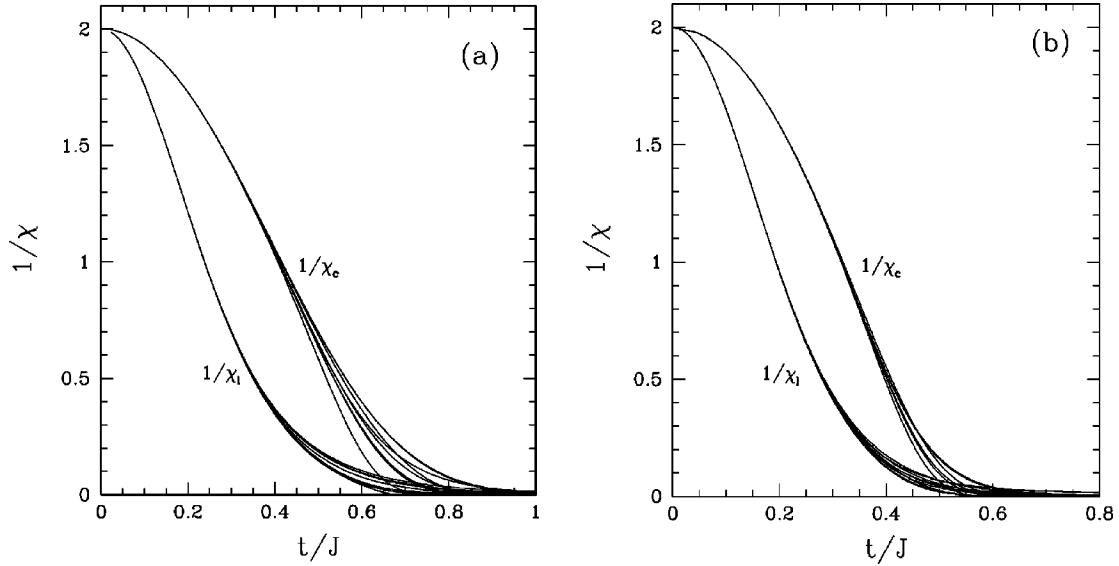


FIG. 6. The inverse antiferromagnetic spin susceptibilities for both local (χ_l) and itinerant spins (χ_c) for the square lattice (a) and for simple cubic lattice (b).

sistent with our estimates above. For the square lattice, our results are in an excellent agreement with the QMC results. For the 3D lattice, we are unaware of any previous results for either energy gap.

IV. SUMMARY AND DISCUSSION

We have used linked-cluster series methods in a comprehensive study of zero-temperature properties of the Kondo lattice model at half filling, for the linear chain, square lattice, and simple cubic lattice. Our work significantly extends a previous series study¹¹ for the ground-state energy and susceptibility, and presents series results for the magnetization, spin and quasiparticle dispersion relations, and energy gaps. Wherever possible we have compared our results with calculations by other methods and, in general, find excellent agreement. It may interest the reader to know that there is

factor of 5×10^4 increase in CPU time to extend the series from λ^8 to λ^{12} .

Our analysis supports the existence of a quantum critical point in the 2D and 3D cases, separating a Kondo spin-liquid phase (large J) from an ordered phase. Our estimates for the critical point are $(t/J) = 0.68 \pm 0.02$, 0.46 ± 0.01 in 2D and 3D cases, respectively. These results are from direct Padé approximants to the series for $\chi^{1/\gamma}$, and hence are biased by, but not particularly sensitive to, the choice of γ . The critical point estimate in 2D agrees very well with previous estimates, while in 3D we find a slightly higher value of $(J/t)_c$, 2.17, compared with 1.833 from mean field.

Our results for the spin and quasiparticle excitation spectra in two and three dimensions suggest that the spin excitation becomes gapless at the quantum critical point, while the charge excitations remain gapped. Thus the appropriate low-energy theory will be the nonlinear sigma model. We have

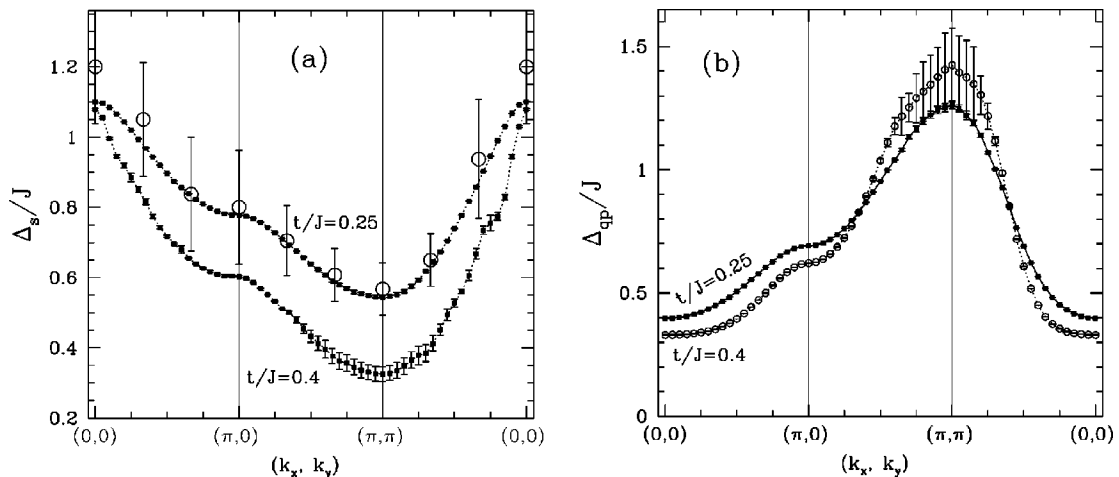


FIG. 7. The triplet spin excitation spectrum (a) and quasiparticle excitation spectrum (b) for the square lattice. The open points with errorbars are variational Monte Carlo results for a 6×6 lattice (Ref. 18).

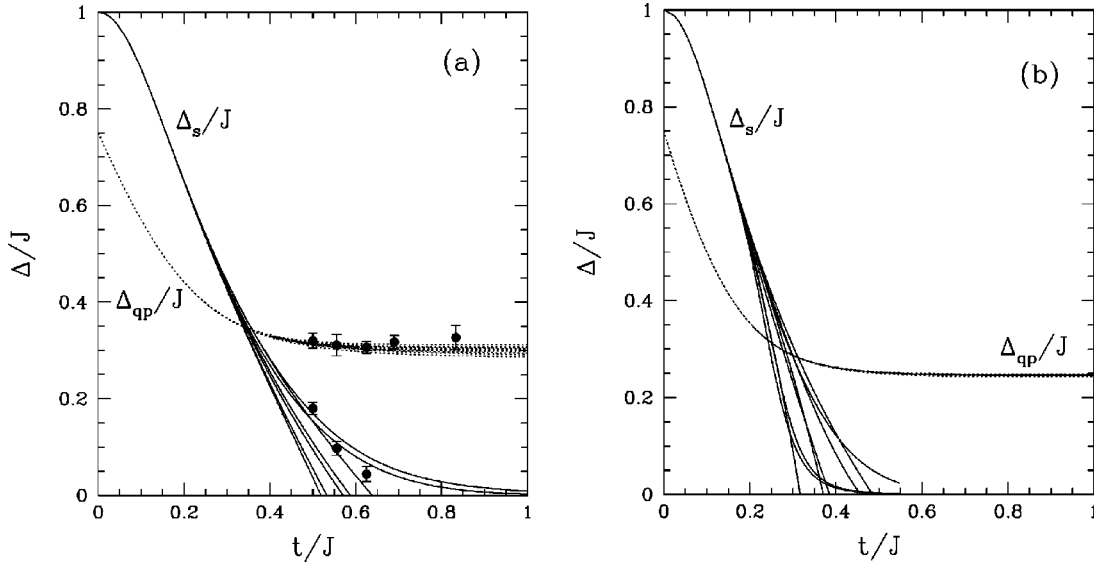


FIG. 8. The triplet spin gap Δ_s/J and quasiparticle gap Δ_{qp}/J for the square lattice (a) and for simple cubic lattice (b) obtained from different orders of integrated differential approximants. The points are the results of the Quantum Monte Carlo study (Ref. 10).

implicitly assumed this in our estimates of the critical points. We have not yet analyzed the data for the frustrated close-packed triangular and face-centered cubic lattices, or for the body-centered cubic lattice, which we have also computed. Nor have we explored the possible existence of bound states, or the region away from half filling. Recent developments in series methods^{19,20} make this possible, and we intend to pursue these directions, as well as others, in future work. Of particular interest, here would be to detect changes in the nature of the quantum critical point with finite doping. Whether this can be done with series methods remains problematic.

After this work was submitted, we learnt of the related, as yet unpublished, work of Trebst *et al.*²¹ Their results appear to agree with our in all the cases where a comparison can be

made. In particular, they agree with our series for the anti-ferromagnetic spin susceptibilities on the simple cubic lattice to their maximum order (λ^{10}), where we had found a discrepancy with Ref. 11.

ACKNOWLEDGMENTS

This work forms part of a research project supported by a grant from the Australian Research Council. The computations were performed on an AlphaServer SC computer. We are grateful for the computing resources provided by the Australian Partnership for Advanced Computing (APAC) National Facility. We thank Simon Trebst for drawing our attention to the work of the Bonn group.

APPENDIX

The dimer series of ground-state energy for 1D KLM are

$$E_0/NJ = -3/4 - 2/3\lambda^2 - 14/45\lambda^4 + 0.71146854791\lambda^6 + 0.19256921565\lambda^8 - 2.8528410569\lambda^{10} + 2.2809484235\lambda^{12} + 12.882850521\lambda^{14} - 30.446998097\lambda^{16} - 43.303667770\lambda^{18} + 270.26259775\lambda^{20} + O(\lambda^{22}). \quad (\text{A1})$$

The triplet spin excitation spectrum for 1D KLM are

$$\begin{aligned} \Delta_s(k)/J = & 1 - \frac{8\lambda^2}{3} + \frac{2356\lambda^4}{135} - 181.93078\lambda^6 + 2152.5066\lambda^8 - 27691.038\lambda^{10} + 329428.5445\lambda^{12} - (2.5917002 \times 10^6)\lambda^{14} \\ & - (2.75912 \times 10^7)\lambda^{16} + (2.23129 \times 10^9)\lambda^{18} + \left(4\lambda^2 - \frac{272\lambda^4}{9} + 305.675\lambda^6 - 4076.18\lambda^8 + 55158.531287\lambda^{10} \right. \\ & \left. - 694363\lambda^{12} + 6.4442 \times 10^6\lambda^{14} + (2.20385 \times 10^7)\lambda^{16} - (3.67419 \times 10^9)\lambda^{18} \right) \cos(k) + \left(\frac{308\lambda^4}{27} - 203.122\lambda^6 \right) \end{aligned}$$

$$\begin{aligned}
& + 3199.476\,135\lambda^8 - 50\,109.7\lambda^{10} + 729\,779.9656\lambda^{12} - (8.927\,78 \times 10^6)\lambda^{14} + (5.423\,26 \times 10^7)\lambda^{16} \\
& + (1.721\,56 \times 10^9)\lambda^{18} \Big) \cos(2k) + [71.0803\lambda^6 - 1809.21\lambda^8 + 35\,912.6434\lambda^{10} - 640789\lambda^{12} \\
& + (1.0026 \times 10^7)\lambda^{14} - (1.220\,82 \times 10^8)\lambda^{16} + (4.1027 \times 10^8)\lambda^{18}] \cos(3k) + [521.400\,048\,9\lambda^8 - 17575\lambda^{10} \\
& + 416\,938.0779\lambda^{12} - (8.345\,62 \times 10^6)\lambda^{14} + (1.409\,49 \times 10^8)\lambda^{16} - (1.770\,87 \times 10^9)\lambda^{18}] \cos(4k) \\
& + [4305.106\lambda^{10} - 178\,962\lambda^{12} + (4.919\,52 \times 10^6)\lambda^{14} - (1.094\,05 \times 10^8)\lambda^{16} + (2.001\,28 \times 10^9)\lambda^{18}] \cos(5k) \\
& + [38\,024.843\lambda^{12} - (1.875\,93 \times 10^6)\lambda^{14} + (5.855\,15 \times 10^7)\lambda^{16} - (1.435\,07 \times 10^9)\lambda^{18}] \cos(6k) \\
& + [351\,790.5722\lambda^{14} - (2.005\,59 \times 10^7)\lambda^{16} + (7.002\,11 \times 10^8)\lambda^{18}] \cos(7k) + [(3.364\,97 \times 10^6)\lambda^{16} \\
& - (2.174\,86 \times 10^8)\lambda^{18}] \cos(8k) + (3.300\,89 \times 10^7)\lambda^{18} \cos(9k). \tag{A2}
\end{aligned}$$

*Electronic address: w.zheng@unsw.edu.au; URL: <http://www.phys.unsw.edu.au/~zwh>

†Electronic address: j.oitmaa@unsw.edu.au

¹G. Aeppli and Z. Fisk, *Comments Condens. Matter Phys.* **16**, 155 (1992).

²P.S. Riseborough, *Adv. Phys.* **49**, 257 (2000).

³E. Dagotto, S. Yunoki, A.L. Malvezzi, A. Moreo, J. Hu, S. Capponi, and D. Poilblanc, *Phys. Rev. B* **58**, 6414 (1998).

⁴H. von Löhneysen, T. Pietrus, G. Portisch, H.G. Schlager, A. Schröder, M. Sieck, and T. Trappman, *Phys. Rev. Lett.* **72**, 3262 (1994); N.D. Mathur, F.M. Grosche, S.R. Julian, I.R. Walker, D.M. Freye, R.K.W. Haselwimmer, and G.G. Lonzarich, *Nature (London)* **394**, 39 (1998).

⁵M. Lavagna and C. Pepin, *Phys. Rev. B* **62**, 6450 (2000).

⁶H. Tsunetsugu, M. Sigrist, and K. Ueda, *Rev. Mod. Phys.* **69**, 809 (1997).

⁷C. Lacroix and M. Cyrot, *Phys. Rev. B* **20**, 1969 (1979).

⁸G.M. Zhang and L. Yu, *Phys. Rev. B* **62**, 76 (2000)

⁹C. Jurecka and W. Brenig, *Phys. Rev. B* **64**, 092406 (2001).

¹⁰F.F. Assaad, *Phys. Rev. Lett.* **83**, 796 (1999); S. Capponi and F.F. Assaad, *Phys. Rev. B* **63**, 155114 (2001).

¹¹Z.P. Shi, R.R.P. Singh, M.P. Gelfand, and Z. Wang, *Phys. Rev. B* **51**, 15630 (1995).

¹²M.P. Gelfand and R.R.P. Singh, *Adv. Phys.* **49**, 93 (2000).

¹³A.J. Guttmann, in “*Phase Transitions and Critical Phenomena*,” edited by C. Domb and J. Lebowitz (New York, Academic, 1989), Vol. 13.

¹⁴M.P. Gelfand, *Solid State Commun.* **98**, 11 (1996).

¹⁵C.C. Yu and S.R. White, *Phys. Rev. Lett.* **71**, 3866 (1993).

¹⁶N. Shibata, T. Nishino, K. Ueda, and C. Ishii, *Phys. Rev. B* **53**, R8828 (1996).

¹⁷Z. Wang, X.P. Li, and D.H. Lee, *Phys. Rev. B* **47**, 11935 (1993).

¹⁸Z. Wang, X.P. Li, and D.H. Lee, *Physica B* **199-200**, 463 (1994).

¹⁹S. Trebst, H. Monien, C.J. Hamer, W.H. Zheng, and R.R.P. Singh, *Phys. Rev. Lett.* **85**, 4373 (2000).

²⁰W.H. Zheng, C.J. Hamer, J. Oitmaa, and R.R.P. Singh, *Phys. Rev. B* **65**, 165117 (2002).

²¹S. Trebst, Ph.D. thesis, University of Bonn, 2002.